

Searching for Dark Photon Tridents Through Primordial Black Hole Signatures

Kingman Cheung,^{1,2,3,*} C.J. Ouseph,^{4,†} Po-Yan Tseng,^{1,2,5,‡} and Sin Kyu Kang^{4,6,§}

¹*Department of Physics, National Tsing Hua University, Hsinchu 30013, Taiwan*

²*Center for Theory and Computation,*

National Tsing Hua University, Hsinchu 30013, Taiwan

³*Division of Quantum Phases and Devices, School of Physics,*

Konkuk University, Seoul 143-701, Republic of Korea

⁴*Institute of Convergence Fundamental Studies,*

Seoul National University of Science and Technology, Seoul 01811, Korea

⁵*Physics Division, National Center for Theoretical Sciences, Taipei 106319, Taiwan*

⁶*School of Natural Science, Seoul National University*

of Science and Technology, Seoul 01811, Korea

(Dated: March 7, 2025)

Abstract

The detection of gamma-ray signals from primordial black holes (PBHs) could provide compelling evidence for their role as a dark matter candidate, particularly through the observation of their Hawking radiation. Future gamma-ray observatories, such as e-ASTROGAM, and the next-generation telescopes, are poised to explore this possibility by measuring both Standard Model (SM) and beyond-the-SM particle emissions. A particularly promising avenue involves production of dark photons by PBHs, which is a hypothetical particle that decays into photons. In this work, we investigate the trident decay of dark photons focusing on their primary emission from PBHs. We assume that the dark photons produced via Hawking radiation decay into photons well before reaching Earth, thereby enhancing the detectable gamma-ray flux. The energy spectrum of the photons decaying from the dark photons is distinct from that of direct Hawking-radiated photons due to higher degree of freedom, leading to observable modifications in the gamma-ray signal. Using the asteroid-mass PBHs as a case study, we demonstrate that future gamma-ray missions could detect dark-photon signatures and distinguish them from conventional Hawking radiation. This approach enables the exploration of previously inaccessible parameter spaces in dark photon mass $m_{A'}$ and their coupling to photons, offering a novel pathway to uncover the properties of dark sectors and the nature of PBHs.

* cheung@phys.nthu.edu.tw

† ouseph444@gmail.com

‡ pytseng@phys.nthu.edu.tw

§ skkang@seoultech.ac.kr

I. INTRODUCTION

Primordial black holes (PBHs) are considered one of the macroscopic dark matter (DM) candidates, accounting for all or a fraction of the cold relic density [1–7]. They can be produced in the early universe through various scenarios: (i) Collapse of overdense regions developed from primordial fluctuations after inflation [8–10], (ii) invoking the first-order phase transitions, accumulating sufficient energy density within the Schwarzschild radius from bubble wall collisions [11–14], and (iii) incorporating dark sector particles in which PBHs are formed from the collapse of the macroscopic intermediate states called fermi-balls [15–18]. Once the PBH mass falls below 10^{-15} solar mass, Hawking radiation becomes significant [19, 20], causing PBHs to emit both Standard Model (SM) and beyond the standard model (BSM) particles. The emitted particle spectra depend only on the PBH temperature and the masses and spins of the particles, regardless of their interaction strengths. Therefore, PBHs are advocated as a candidate for producing feebly-interactive BSM particles, which is difficult to produce or detect in collider experiments. Many earlier works have explored PBH production of DM [21–25], dark radiation [26, 27], axion-like particle (ALP) [28–30], baryon asymmetry in the early universe [31–37].

Based on the current understanding of PBH evaporation, all PBHs with a mass below 10^{15} g would have already evaporated. Therefore, the photon energy spectrum coming off the PBHs peak at about 100 MeV, as the Hawking temperature is inversely proportional to their mass. However, recent literature [38–40] argues that including the back-reaction of emission on the quantum states of the black hole (BH) may modify the standard scenario of Hawking radiation, which is coined as a *memory burden* effect. It is caused by the information stored in the BH, which resists its evaporation. Therefore, once the BH loses a certain fraction of its initial mass, the back-reaction becomes significant enough to suppress or slow down the evaporation process, thereby extending the BH lifetime. Due to the memory burden effect, for example, 10^9 g PBH can still survive to this day. For such a lighter PBH the photon spectrum would be shifted to higher energies.

In this work, we focus on production of dark photons by Hawking radiation from PBHs. The dark photon A' is a hypothetical massive spin-1 particle, which could originate from a $U(1)$ gauge extension of the SM. Through the kinetic mixing with the SM photon, the dark photon weakly couples to other SM particles. When the dark-photon mass exceeds twice

the electron mass, A' decays into a pair of e^+e^- . If the mass is below the e^+e^- threshold, the dark photon decays into 3 photons. This occurs because the tree-level di-photon decay channel is forbidden by the Landau-Yang theorem [41], and so the loop-level photon trident channel $A' \rightarrow 3\gamma$ becomes the dominant one [42]. The three-photon spectrum in this decay is distinguishable from conventional two-body final states. In contrast, this photon-trident signal might not be accessible in collider experiments due to (i) all other existing constraints that force the kinematic mixing ϵ to be too small for practical production and detection, (ii) loop suppression in the trident decay, and (iii) difficulty in resolving 3 photons for dark photon mass below $2m_e$. However, by considering the photon spectrum from the dark photons A' produced by Hawking radiation from PBHs, we can overcome these challenges.

We compute the photon spectrum from PBHs in the region within $|R| < 5^\circ$ of the Galactic Center for two scenarios. We refer to (i) *SM-scenario*, where only SM particles are emitted via the Hawking radiation, and (ii) *dark-photon-scenario*, as the scenario where SM particles and dark photons are emitted via the Hawking radiation. In the SM-scenario, the photon spectrum produced from PBH Hawking radiation includes primary photons, from neutral pion decays, electron final state radiation (FSR), and muon decay+FSR etc. [43]. In the dark-photon-scenario, dark photons are produced in the primary emission from PBHs, and thus the photon-trident spectrum from dark photon decays contributes to the total photon spectrum. We find that the photon spectrum in the dark-photon-scenario can dramatically deviate from that of the SM-scenario when the dark-photon mass is lighter than the PBH temperature. Specifically, we adopt the PBH masses in the range $[10^{15} \text{ g}, 10^{18} \text{ g}]$ and use the sensitivity of e-ASTROGAM [44, 45] to perform the Likelihood analysis. As a result, we are able to identify the parameter space where the dark-photon-scenario can be differentiated from the SM-scenario.

This work is organized as follows. In Section II, we review the dark photon with kinetic mixing to SM photon and formulate the trident-photon decay process. In Section III, we incorporate dark photon into the PBH Hawking radiation and derive the integrated gamma-ray spectrum from the Galactic Center. Section IV utilizes the near future e-ASTROGAM sensitivity to perform a statistical analysis for the identification and discovery potential of the SM scenario and the dark-photon-scenario. Finally, we summarize in Section V.

II. DARK PHOTON MODEL

In this study, we expand the scope of gamma-ray searches for BSM physics, shifting the focus from PBHs alone to including new particles generated by PBHs, with the dark photon serving as a specific example. Specifically, we investigate the signal in the dark-photon-scenario, where dark photons are emitted from PBHs via Hawking radiation, followed by their decays into 3 photons. This process is added to the direct photon emission from PBHs, resulting in a modification of the total spectrum. We then contrast this signal with the SM-scenario in which PBHs produce only SM particles. Since observations of galactic gamma-ray signals impose stricter constraints on PBH abundance compared to studies of dwarf spheroidal galaxies [46], we concentrate on the Milky Way’s gamma-ray signal for the dark-photon-scenario.

Dark Photon Trident. — The Lagrangian for the dark photon A' with mass $m_{A'}$ and for kinematic mixing with the SM photon is described by

$$\mathcal{L} \supset -\frac{1}{4}F'_{\mu\nu}F'^{\mu\nu} - \frac{1}{2}m_{A'}^2 A'_\mu A'^\mu - \frac{\epsilon}{2}F'_{\mu\nu}F^{\mu\nu}, \quad (1)$$

where the field strength tensor for the dark photon is defined as $F'_{\mu\nu} = \partial_\mu A'_\nu - \partial_\nu A'_\mu$, and $F^{\mu\nu}$ is the field strength for the SM photon. The presence of a nonzero kinetic mixing parameter ϵ allows the dark photon to interact with other SM particles via mixing with the photon.

For the dark photon mass below twice the electron mass, the dominant decay mode is into three photons, a process termed the dark-photon trident. The only other kinematically feasible decay channel is into a neutrino pair, arising from dark-photon mixing with the SM Z boson [42, 47–50]. However, due to the large mass of the Z boson, this decay is severely suppressed and thus neglected in this analysis. Earlier studies computed the rate of this three-photon decay using an Effective Field Theory (EFT) approach, which is valid in the limit where the dark-photon mass is much smaller than the electron mass [51, 52]. By integrating out heavy fermions at one-loop, the resulting effective Lagrangian follows the Euler-Heisenberg form:

$$\mathcal{L}_{A'}^{\text{EH}} = \frac{\epsilon\alpha_{\text{em}}}{45m_e^4} \left(14F'_{\mu\nu}F^{\nu\lambda}F_{\lambda\rho}F^{\rho\mu} - 5F'_{\mu\nu}F^{\mu\nu}F_{\alpha\beta}F^{\alpha\beta} \right), \quad (2)$$

	c_k	$c_k \times 4^k$
c_1	335 / 714	1.88
c_2	128,941 / 839,664	2.46
c_3	44,787 / 1,026,256	2.79
c_4	1,249,649,333 / 108,064,756,800	5.92
c_5	36,494,147 / 12,382,420,050	3.02
c_6	867,635,449 / 1,614,300,688,000	2.20

TABLE I: Coefficients in the expansion of the decay process $A' \rightarrow \gamma\gamma\gamma$ for a dark photon mass below twice the electron mass. The expansion is considered up to the sixth order in the calculation of the total decay width under the Euler-Heisenberg limit [54].

which leads to the decay width in the Euler-Heisenberg limit [53]:

$$\begin{aligned} \Gamma_{\text{EH}} &= \frac{17\epsilon^2\alpha_{\text{em}}^4}{11664000\pi^3} \times \frac{m_{A'}^9}{m_e^8} \\ &\simeq 1\text{s}^{-1} \times \left(\frac{\epsilon}{0.003}\right)^2 \times \left(\frac{m_{A'}}{m_e}\right)^9. \end{aligned} \quad (3)$$

Nevertheless, the validity of the EFT approach deteriorates for $m_{A'} \sim m_e$. To account for corrections beyond the Euler-Heisenberg limit, the full decay width can be expressed as [54]:

$$\Gamma_{A' \rightarrow 3\gamma} = \Gamma_{\text{EH}} \left[1 + \sum_{k=1}^{\infty} c_k \left(\frac{m_{A'}^2}{m_e^2}\right)^k \right]. \quad (4)$$

Here, the expansion consists of the series of coefficients c_k , with values that are shown in Table I up to order 6. Previous studies have shown that loop corrections can enhance the decay rate by up to two orders of magnitude when $m_{A'}$ approaches twice the electron mass.

The energy spectrum of photons produced in dark-photon trident decay is given by [50, 53]:

$$\frac{dN_\gamma}{dE_\gamma} = \frac{2x^3}{17m_{A'}} \left(1715 - 3105x + \frac{2919}{2}x^2 \right), \quad (5)$$

where $x = 2E_\gamma/m_{A'}$ varies between 0 and 1.

The kinematic distribution of the dark photon in the laboratory(lab) frame can be obtained using the following formula [55].

$$\frac{dN'_\gamma}{dE'_\gamma} = \frac{1}{2} \int dE_\gamma d\cos\theta \frac{dN_\gamma}{dE_\gamma} \delta(E'_\gamma - \gamma(E_\gamma + \beta p \cos\theta)), \quad (6)$$

$$= \frac{1}{2} \int_{E'_1}^{E'_2} dE'_\gamma \frac{dN_\gamma}{dE'_\gamma} \frac{1}{p\beta\gamma}, \quad (7)$$

where $E'_2 = \gamma(E'_\gamma + p'\beta)$ and $E'_1 = \gamma(E'_\gamma - p'\beta)$ and the prime variables refer to those in the lab frame. This formula allows us to obtain the boosted spectrum from the decay spectrum at rest.

III. HAWKING RADIATION EMISSION FROM PRIMORDIAL BLACK HOLES

A BH is predicted to continuously emit particles near its event horizon, a phenomenon known as Hawking radiation [57]. In this section, we discuss the particle spectra associated with Hawking radiation [46]. Particles emitted directly from the BH are referred to as primary particles, whereas those resulting from interactions of primary particles are termed secondary particles. The production rate of a primary particle i per unit time and energy from a BH of mass M is given by [57–59]:

$$\frac{\partial N_{i,\text{primary}}}{\partial E_i \partial t} = \frac{g_i}{2\pi} \frac{\Gamma_i(E_i, M, m_i)}{e^{E_i/T_H} \pm 1}, \quad (8)$$

where m_i and g_i represent the mass and degrees of freedom of the particle i , Γ_i is the greybody factor, and $T_H = 1/(8\pi GM)$ is the Hawking temperature. The plus and minus signs correspond to fermions and bosons, respectively. At high energies, the greybody factor approaches the geometrical optics limit, $\Gamma_i = 27G^2 M^2 E_i^2$. The greybody factor Γ_i is computed using the `BlackHawk` package [43, 60]. The particle rest mass imposes a cutoff on the evaporation spectrum for $E_i < m_i$. Note that the greybody factor used in `BlackHawk` assumes the production of massless particles. However, this should have a minimal effect on our results, except in the case where $m_{A'} \gg T_H$.

We focus on the photon spectrum of Hawking radiation, which includes contributions from both primary photons and secondary photons produced via decays and final-state radiation (FSR) of primary particles. The total photon spectrum is expressed as:

$$\begin{aligned} \frac{\partial N_{\gamma,\text{tot}}}{\partial E_\gamma \partial t} &= \frac{\partial N_{\gamma,\text{primary}}}{\partial E_\gamma \partial t} + \int dE_{A'} \frac{\partial N_{A',\text{primary}}}{\partial E_{A'} \partial t} \frac{dN_{A',\text{decay}}}{dE_\gamma} \\ &+ \int dE_{\pi^0} 2 \frac{\partial N_{\pi^0,\text{primary}}}{\partial E_{\pi^0} \partial t} \frac{dN_{\pi^0,\text{decay}}}{dE_\gamma} \\ &+ \sum_{i=e^\pm, \mu^\pm, \pi^\pm} \int dE_i \frac{\partial N_{i,\text{primary}}}{\partial E_i \partial t} \frac{dN_{i,\text{FSR}}}{dE_\gamma}. \end{aligned} \quad (9)$$

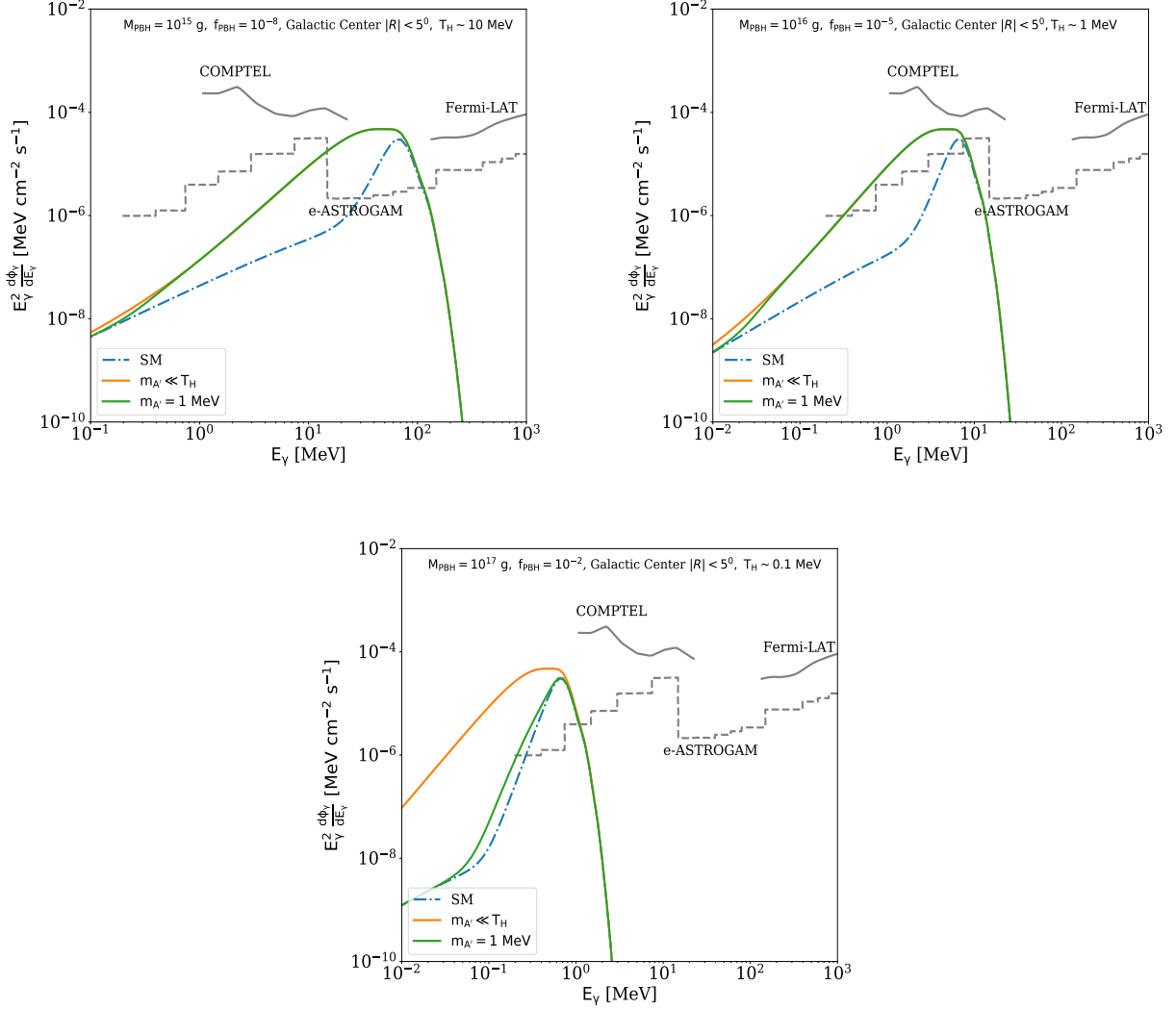


FIG. 1: Gamma-ray spectra from Hawking radiation for PBHs with $(M_{\text{PBH}}, f_{\text{PBH}}) = (10^{15} \text{ g}, 10^{-8})$ in the top-left panel, $(10^{16} \text{ g}, 10^{-5})$ in the top-right, and $(10^{17} \text{ g}, 10^{-2})$ in the bottom-center. The spectra include the SM-scenario (dotted-dashed blue) and the dark-photon-scenario for different dark photon masses (various colors). The region of interest (ROI) is the Galactic center with $|R| \leq 5^\circ$. Experimental constraints and future sensitivities are shown for COMPTEL (solid), Fermi-LAT [56] (solid), and e-ASTROGAM [44, 45] (dashed).

where:

$$\frac{dN_{\pi^0, \text{decay}}}{dE_\gamma} = \frac{\Theta(E_\gamma - E_{\pi^0}^-)\Theta(E_{\pi^0}^+ - E_\gamma)}{E_{\pi^0}^+ - E_{\pi^0}^-}, \quad (10)$$

$$E_{\pi^0}^\pm = \frac{1}{2} \left(E_{\pi^0} \pm \sqrt{E_{\pi^0}^2 - m_{\pi^0}^2} \right), \quad (11)$$

and

$$\frac{dN_{i, \text{FSR}}}{dE_\gamma} = \frac{\alpha}{\pi Q_i} P_{i \rightarrow i\gamma}(x) \left[\log \left(\frac{1-x}{\mu_i^2} \right) - 1 \right], \quad (12)$$

$$P_{i \rightarrow i\gamma}(x) = \begin{cases} \frac{2(1-x)}{x}, & i = \pi^\pm \\ \frac{1+(1-x)^2}{x}, & i = \mu^\pm, e^\pm \end{cases}. \quad (13)$$

where $x = \frac{2E_\gamma}{Q_i}$, $\mu_i = \frac{m_i}{Q_i}$, and $Q_i = 2E_i$. Note that we ignore the three-body decay of μ^\pm and π^\pm . These processes can be safely neglected because their masses are much larger than the energy range of interest.

On the other hand, the energy spectrum of photons produced in dark-photon trident decay is given in Eq. [5-7].

The photon flux observed near Earth is given by:

$$\frac{d\Phi_\gamma}{dE_\gamma} = \bar{J}_D \frac{\Delta\Omega}{4\pi} \int dM \frac{f_{\text{PBH}}(M)}{M} \frac{\partial N_{\gamma, \text{tot}}}{\partial E_\gamma \partial t}, \quad (14)$$

where \bar{J}_D is the J-factor for decay, defined as:

$$\bar{J}_D = \frac{1}{\Delta\Omega} \int_{\Delta\Omega} d\Omega \int_{\text{LOS}} dl \rho_{\text{DM}}. \quad (15)$$

The dark matter distribution in the Milky Way halo is modeled using a Navarro–Frenk–White (NFW) profile [61]:

$$\rho_{\text{DM}}(r) = \frac{\rho_s}{\frac{r}{r_s} \left(1 + \frac{r}{r_s}\right)^2} \Theta(r_{200} - r), \quad (16)$$

with parameters $r_s = 11$ kpc, $\rho_s = 0.838$ GeV/cm³, $r_{200} = 193$ kpc, and $r_\odot = 8.122$ kpc [62]. For a region of interest (ROI) within $|R| < 5^\circ$ of the Galactic Center, the J-factor is $\bar{J}_D = 1.597 \times 10^{26}$ MeVcm⁻²sr⁻¹, and the angular size is $\Delta\Omega = 2.39 \times 10^{-2}$ sr.

In this study, we consider a monochromatic PBH mass distribution, which can arise, for instance, from the collapse of Q-balls [63] or a first-order phase transition [64]. Assuming $f_{\text{PBH}}(M) = f_{\text{PBH}} \delta(M - M_{\text{PBH}})$ Eq. (14) simplifies to

$$\frac{d\Phi_\gamma}{dE_\gamma} = \bar{J}_D \frac{\Delta\Omega}{4\pi} \frac{f_{\text{PBH}}}{M_{\text{PBH}}} \frac{\partial N_{\gamma, \text{tot}}}{\partial E_\gamma \partial t}. \quad (17)$$

In the dark-photon-scenario, the gamma-ray spectrum arises from two contributions: (i) direct photon emission from PBHs and (ii) secondary emission resulting from dark-photon decays. Figure 1 illustrates the photon spectrum for this scenario, considering PBH masses of $M_{\text{PBH}} = 10^{15}$, 10^{16} , and 10^{17} g, PBH abundance fractions of $f_{\text{PBH}} = 10^{-8}$, 10^{-5} , and 10^{-2} , and a range of dark-photon masses.

The energy of photons produced from dark-photon decays (E_γ) is typically lower than the initial dark-photon energy ($E_{A'}$). Furthermore, the production of dark photons with masses significantly exceeding the primary photon peak is suppressed. As a result, the visible dark-photon peak always appears to the left of the primary photon peak. The dark-photon spectrum exhibits a distinct peak location and spectral shape compared to the photon spectrum in the SM-scenario.

A. Dark Photon Parameter Space

For dark photons to alter the photon spectrum near the Earth, they must decay before arriving. The probability of dark photons decaying during their propagation from the Galactic center to Earth, assuming a monochromatic PBH mass, is given by [66]

$$\langle P_{A',\text{decay}} \rangle \equiv \frac{\Phi_{A',\text{dec}}}{\Phi_{A',\text{tot}}}, \quad (18)$$

where

$$\Phi_{A',\text{tot}} = \int_{\Delta\Omega} \frac{d\Omega}{4\pi} \int_{\text{LOS}} d\ell \int dE_{A'} \frac{f_{\text{PBH}}\rho_{\text{DM}}}{M_{\text{PBH}}} \frac{\partial N_{A',\text{primary}}}{\partial E_{A'}\partial t} = \bar{J}_D \frac{\Delta\Omega}{4\pi} \frac{f_{\text{PBH}}}{M_{\text{PBH}}} \int dE_{A'} \frac{\partial N_{A',\text{primary}}}{\partial E_{A'}\partial t} \quad (19)$$

$$\Phi_{A',\text{dec}} = \int_{\Delta\Omega} \frac{d\Omega}{4\pi} \int_{\text{LOS}} d\ell \int dE_{A'} \frac{f_{\text{PBH}}\rho_{\text{DM}}}{M_{\text{PBH}}} \frac{\partial N_{A',\text{primary}}}{\partial E_{A'}\partial t} P_{A',\text{decay}}(E_{A'}, \ell). \quad (20)$$

The decay probability $P_{A',\text{decay}}$ is given by [66]

$$P_{A',\text{decay}}(E_{A'}, D) = 1 - \exp\left(-D \Gamma_{A' \rightarrow 3\gamma} \frac{m_{A'}}{\sqrt{E_{A'}^2 - m_{A'}^2}}\right), \quad (21)$$

where $E_{A'}$ is a nearly thermal energy distribution and D is the distance traveling from the PBH.

We require $\langle P_{A',\text{decay}} \rangle$ to be greater than 99% to determine the regions above the color curves in Fig. 2 as viable (For each $m_{A'}$, the minimum ϵ that satisfies $P_{\text{decay}} \geq 99\%$ is determined.). For most of the parameter regions shown in Fig. 2, we assume the dark-photon decay is

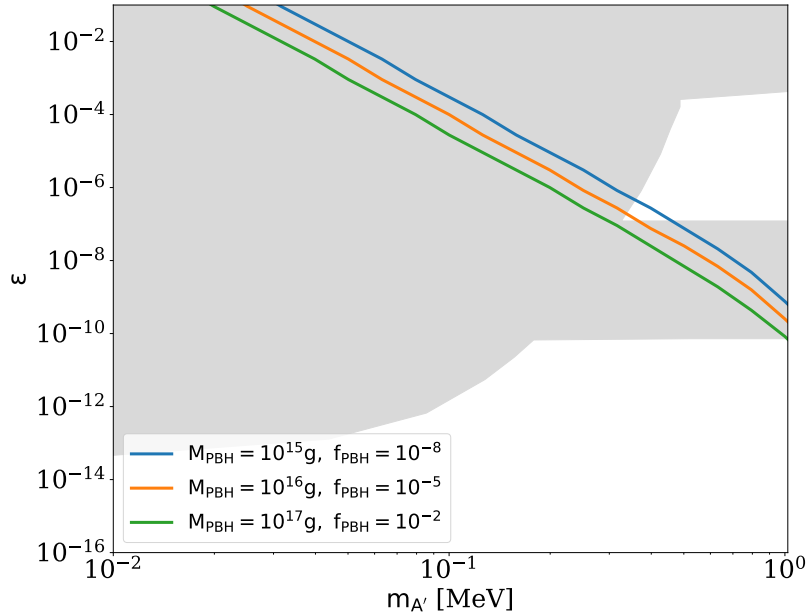


FIG. 2: The parameter space for dark photons that can be explored using PBHs is presented. The chosen PBH parameters are: $M_{\text{PBH}} = 10^{15} \text{ g}$, $f_{\text{PBH}} = 10^{-8}$ (blue); $M_{\text{PBH}} = 10^{16} \text{ g}$, $f_{\text{PBH}} = 10^{-5}$ (orange); and $M_{\text{PBH}} = 10^{17} \text{ g}$, $f_{\text{PBH}} = 10^{-2}$ (green). Regions above the color curves are viable and existing constraints (gray) are taken from Ref. [65].

prompt since ϵ is at least one order of magnitude larger than the lower boundaries, which correspond to the color curves. Since the decay width of dark photons is proportional to the square of the coupling, it follows that $\Gamma_{A' \rightarrow 3\gamma} \propto \epsilon^2$. For the evaluation of $\Phi_{A', \text{dec}}$ we assume that most of the dark photons originate from the Galactic center¹. It is worth mentioning that, comparing with existing constraints (gray area in Fig. 2), this PBH dark-photon-scenario can probe the unexplored parameter space $10^{-7} \leq \epsilon \leq 10^{-3}$ and $m_{A'} \geq 0.5 \text{ MeV}$, i.e. the white trapezoidal area in Fig. 2, for which the A' decay length is too long for terrestrial experiments meanwhile the mean free path is too short to escape from SN1987A. As a result, the PBH dark-photon-scenario provides a complementary sensitivity for dark photon.

¹ D in Eq. 21 is fixed as the distance between the galactic center and Earth, approximately 8.3 kiloparsecs, which corresponds to a light travel time of 8.53×10^{11} seconds. This is calculated using the speed of light ($c = 3 \times 10^8 \text{ m/s}$) and $1 \text{ parsec} \approx 3.086 \times 10^{16} \text{ m}$.

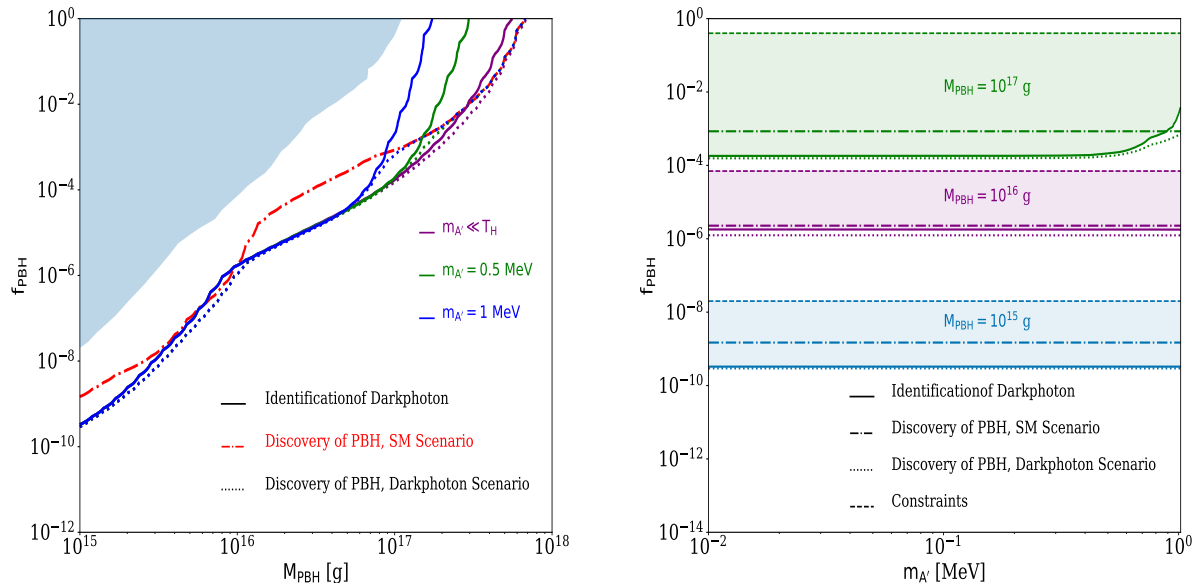


FIG. 3: Bounds on PBH differentiability in the f_{PBH} vs. M_{PBH} plane (left) and the f_{PBH} vs. $m_{A'}$ plane (right). The curves represent the ability to differentiate between a PBH signal in the SM-scenario (dotted-dash) and the dark-photon-scenario (dotted) from the background. Additionally, the distinguishability between the dark-photon-scenario and the SM-scenario is shown (solid), along with past experimental constraints (left: shaded light blue and right: dashed). In the $m_{A'}$ plane, the shaded region indicates the parameter space where the dark-photon-scenario signal can be distinguished from the SM-scenario signal, with the far-right edge representing the maximum allowed $m_{A'}$.

IV. RESULTS & DISCUSSION

We use the likelihood analysis to constrain a specific model, assuming a Reference model that generates an observable gamma-ray signal [45, 66], which, in our case, corresponds to the astrophysical background given by experiments. A Test model with inputs from the new physics is then evaluated against the Reference model. In our study, we consider two test models for PBH (i) the SM-scenario and (ii) the dark-photon-scenario. The probability that the Test model reproduces the gamma-ray signal predicted by the Reference model follows

the Poisson statistics represented as

$$\mathcal{L} = \exp \left(\sum_i n_i \ln \sigma_i - \sigma_i - \ln n_i! \right), \quad (22)$$

where n_i denotes the observed photon counts from the Reference model, incorporating any background contributions, and σ_i represents the expected photon count from the Test model including background within the i -th energy bin. To assess the relative validity of different Test models, the test statistic (TS) is introduced, defined as

$$\text{TS} = -2 \ln \left(\frac{\mathcal{L}}{\mathcal{L}_{\text{Ref}}} \right) = \Sigma^2, \quad (23)$$

where Σ corresponds to the observational significance [67–70], and \mathcal{L}_{Ref} is the likelihood associated with the Reference model. This analysis assumes that the combined statistical evaluation across gamma-ray energy bins follows a χ^2 distribution. Unless stated otherwise, a significance threshold of $\Sigma = 3$ is adopted.

The construction of both the Reference and Test signals, along with the estimated background, is based on gamma-ray emission from the region around the Galactic Center, modeled using the Navarro-Frenk-White (NFW) density profile within a 5° field of view. The expected detector sensitivity and instrumental response are incorporated based on the design specifications of next-generation gamma-ray observatories. Additionally, forecasts of the astrophysical background are included to ensure a realistic evaluation of the observational prospects[44, 45].²

A. Identifying Signals and Differentiating Standard Model Processes from Dark Photon Interactions

To evaluate the detectability of a given model (PBH in the SM-scenario or PBH in dark-photon-scenario), we perform the aforementioned analysis, considering the astrophysical background as the Reference model. Subsequently, we systematically scan the parameter space of the Test model to determine the values at which the likelihood deviates beyond a predefined significance level. The resulting constraints establish the PBH discovery limits, as depicted in Fig. 3. If the PBH population exceeds the corresponding threshold, the emitted signals will be sufficiently luminous to be detected above the background.

² Please refer to Ref. [44, 45, 66] for more details about the detector sensitivity and foreground used.

It is crucial to emphasize that for fixed M_{PBH} and $m_{A'}$, the constraints in the dark-photon-scenario are at least as stringent as those in the SM-scenario. This is because PBHs produce the same SM particles, while the presence of dark photons introduces additional degrees of freedom (d.o.f =3 for dark photon), leading to an overall enhancement in signal brightness and detectability. Nevertheless, for heavier PBHs or heavier dark photons, the constraints in the dark-photon-scenario asymptotically approach those of the SM-scenario. This transition occurs because the contribution from dark photons experiences exponential suppression when the Hawking temperature significantly falls below $m_{A'}$.

In the $(M_{\text{PBH}}, f_{\text{PBH}})$ plane presented in Fig. 3, the region above the solid curves delineates the parameter space where the dark-photon induced signal can be distinguished from the SM-scenario (i.e., the astrophysical background plus the SM-scenario as the Reference model). Additionally, the figure illustrates the lower bounds on f_{PBH} required to differentiate a PBH signal from the background, with dotted lines representing the dark-photon-scenario and dot-dashed lines corresponding to the SM-scenario. As expected, the threshold for distinguishing the dark-photon-scenario from the SM-scenario is always higher than the detection threshold for the dark-photon signal itself, since the presence of a detectable signal is a prerequisite for further characterization. Furthermore, the identification threshold for the dark-photon signal remains consistently lower than that of the SM-scenario due to its enhanced luminosity.

A notable feature is that for sufficiently large M_{PBH} , the identification lines for the dark-photon and SM scenarios converge. This convergence arises because dark photons become exponentially suppressed when the Hawking temperature drops below their mass, rendering their contribution negligible. Consequently, the distinguishability limits rapidly lose sensitivity, as the dark photon and SM signals become nearly indistinguishable. An additional factor contributing to this effect is the experimental sensitivity: at high PBH masses, the signal may extend beyond the detector's range, whereas in certain cases, additional photons from dark-photon decays may populate regions of low detector sensitivity. For reference, existing PBH constraints in the SM case from Refs. [7, 46, 71] are also included.

In the $(m_{A'}, f_{\text{PBH}})$ plane of Fig. 3, the line styles remain consistent with those in the left panel. Solid curves denote the distinguishability limits between the dark photon and SM scenarios, whereas dotted lines represent the discovery limits for differentiating a PBH signal from the background in the presence of dark photons. For small $m_{A'}$, these curves remain relatively flat, as dark photons behave effectively as massless particles due to their high

energies. Conversely, for large $m_{A'}$, they transit to a nonrelativistic regime and undergo exponential suppression once the Hawking temperature falls below their mass. Consequently, the background identification threshold saturates, aligning with the SM-scenario identification curve (dot-dashed).

In contrast, the distinguishability curve between the dark photon and SM scenarios rises steeply at large $m_{A'}$ due to the diminishing contrast between the two signals. Additionally, existing constraints on PBHs in the SM-scenario are depicted using dashed lines, indicating the region above which PBHs in the SM-scenario have already been excluded. The shaded regions highlight the viable parameter space where the dark-photon-scenario remains distinguishable from the SM-scenario.

V. CONCLUSION

This study has investigated the detectability of gamma-ray signals from PBHs, with a particular focus on the emission of dark photons via Hawking radiation. By analyzing the trident decay of dark photons, we establish that these events lead to distinct gamma-ray signatures, providing a means to differentiate the scenario from the conventional Hawking radiation. Our results indicate that future gamma-ray observatories, such as e-ASTROGAM, may be capable of probing previously unexplored regions of the dark-photon parameter space using asteroid-mass PBHs as a benchmark scenario.

The study has further demonstrated that the presence of dark photons enhances the gamma-ray flux, thereby improving the detectability of PBH signals. The influence of spin-dependent greybody factors significantly alters the energy spectrum of the emitted photons, contributing to observable modifications in the gamma-ray signal. This effect enables a clear distinction between PBH emissions within the SM and those incorporating dark photons, reinforcing their viability as probes of the dark sector.

Furthermore, we show that the constraints imposed by dark photon emission are generally stronger than those from the SM scenario, except in the limit of large PBH masses or heavy dark photons, for which the signals converge due to exponential suppression. These findings offer a compelling case for future experimental efforts to search for dark photons in PBH emissions, presenting a novel pathway to explore new physics BSM.

Overall, this work provides a crucial step toward understanding the interplay between

PBHs, dark photons, and the nature of dark matter. Future observational missions will be instrumental in testing these predictions, potentially uncovering signatures of new physics that extend beyond current theoretical frameworks.

ACKNOWLEDGMENT

Special thanks to Yuhsin Tsai for the early discussions on gamma-ray spectrum-related calculations and to Nguyen Tran Quang Thong for valuable discussions. K.C. is supported by the National Science & Technology Council under grant no. NSTC 113-2112-M-007-041-MY3. C. J. O. and S. K. K are supported by the National Research Foundation of Korea under grant NRF-2023R1A2C100609111. P. Y. Tseng is supported in part by the National Science and Technology Council with Grant No. NSTC-111-2112-M-007-012-MY3, and Physics Division of the National Center for Theoretical Sciences of Taiwan with Grant NSTC 114-2124-M-002-003.

-
- [1] S. Hawking, *Mon. Not. Roy. Astron. Soc.* **152**, 75 (1971).
 - [2] G. F. Chapline, *Nature* **253**, 251 (1975).
 - [3] M. Y. Khlopov, *Res. Astron. Astrophys.* **10**, 495 (2010), [arXiv:0801.0116 \[astro-ph\]](#).
 - [4] B. Carr, F. Kuhnel, and M. Sandstad, *Phys. Rev. D* **94**, 083504 (2016), [arXiv:1607.06077 \[astro-ph.CO\]](#).
 - [5] B. Carr, K. Kohri, Y. Sendouda, and J. Yokoyama, *Rept. Prog. Phys.* **84**, 116902 (2021), [arXiv:2002.12778 \[astro-ph.CO\]](#).
 - [6] B. Carr and F. Kuhnel, *Ann. Rev. Nucl. Part. Sci.* **70**, 355 (2020), [arXiv:2006.02838 \[astro-ph.CO\]](#).
 - [7] A. M. Green and B. J. Kavanagh, *J. Phys. G* **48**, 043001 (2021), [arXiv:2007.10722 \[astro-ph.CO\]](#).
 - [8] B. J. Carr and S. W. Hawking, *Mon. Not. Roy. Astron. Soc.* **168**, 399 (1974).
 - [9] M. Sasaki, T. Suyama, T. Tanaka, and S. Yokoyama, *Class. Quant. Grav.* **35**, 063001 (2018), [arXiv:1801.05235 \[astro-ph.CO\]](#).

- [10] K. Cheung, C. J. Ouseph, and P.-Y. Tseng, *Eur. Phys. J. C* **84**, 906 (2024), [arXiv:2307.08046 \[hep-ph\]](#).
- [11] S. W. Hawking, I. G. Moss, and J. M. Stewart, *Phys. Rev. D* **26**, 2681 (1982).
- [12] H. Kodama, M. Sasaki, and K. Sato, *Prog. Theor. Phys.* **68**, 1979 (1982).
- [13] I. G. Moss, *Phys. Rev. D* **50**, 676 (1994).
- [14] R. V. Konoplich, S. G. Rubin, A. S. Sakharov, and M. Y. Khlopov, *Phys. Atom. Nucl.* **62**, 1593 (1999).
- [15] M. J. Baker, M. Breitbach, J. Kopp, and L. Mittnacht, (2021), [arXiv:2105.07481 \[astro-ph.CO\]](#).
- [16] C. Gross, G. Landini, A. Strumia, and D. Teresi, *JHEP* **09**, 033 (2021), [arXiv:2105.02840 \[hep-ph\]](#).
- [17] K. Kawana and K.-P. Xie, *Phys. Lett. B* **824**, 136791 (2022), [arXiv:2106.00111 \[astro-ph.CO\]](#).
- [18] D. Marfatia and P.-Y. Tseng, *JHEP* **08**, 001 (2022), [Erratum: *JHEP* **08**, 249 (2022)], [arXiv:2112.14588 \[hep-ph\]](#).
- [19] S. W. Hawking, *Commun. Math. Phys.* **43**, 199 (1975), [Erratum: *Commun.Math.Phys.* **46**, 206 (1976)].
- [20] G. W. Gibbons and S. W. Hawking, *Phys. Rev. D* **15**, 2738 (1977).
- [21] N. F. Bell and R. R. Volkas, *Phys. Rev. D* **59**, 107301 (1999), [arXiv:astro-ph/9812301](#).
- [22] R. Allahverdi, J. Dent, and J. Osinski, *Phys. Rev. D* **97**, 055013 (2018), [arXiv:1711.10511 \[astro-ph.CO\]](#).
- [23] O. Lennon, J. March-Russell, R. Petrossian-Byrne, and H. Tillim, *JCAP* **04**, 009 (2018), [arXiv:1712.07664 \[hep-ph\]](#).
- [24] D. Marfatia and P.-Y. Tseng, *JHEP* **04**, 006 (2023), [arXiv:2212.13035 \[hep-ph\]](#).
- [25] T. Kim, P. Lu, D. Marfatia, and V. Takhistov, *Phys. Rev. D* **110**, L051702 (2024), [arXiv:2309.05703 \[hep-ph\]](#).
- [26] A. Arbey, J. Auffinger, P. Sandick, B. Shams Es Haghi, and K. Sinha, *Phys. Rev. D* **103**, 123549 (2021), [arXiv:2104.04051 \[astro-ph.CO\]](#).
- [27] I. Masina, *Grav. Cosmol.* **27**, 315 (2021), [arXiv:2103.13825 \[gr-qc\]](#).
- [28] F. Schiavone, D. Montanino, A. Mirizzi, and F. Capozzi, *JCAP* **08**, 063 (2021), [arXiv:2107.03420 \[hep-ph\]](#).

- [29] N. Bernal, F. Hajkarim, and Y. Xu, *Phys. Rev. D* **104**, 075007 (2021), [arXiv:2107.13575 \[hep-ph\]](#).
- [30] K. Mazde and L. Visinelli, *JCAP* **01**, 021 (2023), [arXiv:2209.14307 \[astro-ph.CO\]](#).
- [31] B. J. Carr, *Astrophys. J.* **206**, 8 (1976).
- [32] D. Toussaint, S. B. Treiman, F. Wilczek, and A. Zee, *Phys. Rev. D* **19**, 1036 (1979).
- [33] M. S. Turner, *Phys. Lett. B* **89**, 155 (1979).
- [34] D. Baumann, P. J. Steinhardt, and N. Turok, (2007), [arXiv:hep-th/0703250](#).
- [35] T. Fujita, M. Kawasaki, K. Harigaya, and R. Matsuda, *Phys. Rev. D* **89**, 103501 (2014), [arXiv:1401.1909 \[astro-ph.CO\]](#).
- [36] A. Hook, *Phys. Rev. D* **90**, 083535 (2014), [arXiv:1404.0113 \[hep-ph\]](#).
- [37] D. Hooper and G. Krnjaic, *Phys. Rev. D* **103**, 043504 (2021), [arXiv:2010.01134 \[hep-ph\]](#).
- [38] G. Dvali, (2018), [arXiv:1810.02336 \[hep-th\]](#).
- [39] G. Dvali, L. Eisemann, M. Michel, and S. Zell, *Phys. Rev. D* **102**, 103523 (2020), [arXiv:2006.00011 \[hep-th\]](#).
- [40] G. Dvali, J. S. Valbuena-Bermúdez, and M. Zantedeschi, *Phys. Rev. D* **110**, 056029 (2024), [arXiv:2405.13117 \[hep-th\]](#).
- [41] C. N. Yang, *Phys. Rev.* **77**, 242 (1950).
- [42] T. Linden, T. T. Q. Nguyen, and T. M. P. Tait, (2024), [arXiv:2406.19445 \[hep-ph\]](#).
- [43] A. Arbey and J. Auffinger, *Eur. Phys. J. C* **81**, 910 (2021), [arXiv:2108.02737 \[gr-qc\]](#).
- [44] A. De Angelis et al. (e-ASTROGAM), *Exper. Astron.* **44**, 25 (2017), [arXiv:1611.02232 \[astro-ph.HE\]](#).
- [45] K. Agashe, J. H. Chang, S. J. Clark, B. Dutta, Y. Tsai, and T. Xu, *Phys. Rev. D* **105**, 123009 (2022), [arXiv:2202.04653 \[astro-ph.CO\]](#).
- [46] A. Coogan, L. Morrison, and S. Profumo, *Phys. Rev. Lett.* **126**, 171101 (2021), [arXiv:2010.04797 \[astro-ph.CO\]](#).
- [47] T. T. Q. Nguyen and T. M. P. Tait, *Phys. Rev. D* **107**, 115016 (2023), [arXiv:2212.12547 \[hep-ph\]](#).
- [48] T. T. Q. Nguyen, in [Windows on the Universe: 30th Anniversary of the Rencontres du Vietnam](#) (2023) [arXiv:2312.12292 \[hep-ph\]](#).
- [49] T. T. Q. Nguyen, I. John, T. Linden, and T. M. P. Tait, (2024), [arXiv:2412.00180 \[hep-ph\]](#).
- [50] T. Linden, T. T. Q. Nguyen, and T. M. P. Tait, (2024), [arXiv:2402.01839 \[hep-ph\]](#).

- [51] M. Pospelov, *Phys. Rev. D* **80**, 095002 (2009), [arXiv:0811.1030 \[hep-ph\]](#).
- [52] J. Redondo and M. Postma, *JCAP* **02**, 005 (2009), [arXiv:0811.0326 \[hep-ph\]](#).
- [53] M. Pospelov, A. Ritz, and M. B. Voloshin, *Phys. Lett. B* **662**, 53 (2008), [arXiv:0711.4866 \[hep-ph\]](#).
- [54] S. D. McDermott, H. H. Patel, and H. Ramani, *Phys. Rev. D* **97**, 073005 (2018), [arXiv:1705.00619 \[hep-ph\]](#).
- [55] D. Berger, A. Rajaraman, and J. Kumar, *Pramana* **94**, 133 (2020), [arXiv:1903.10632 \[hep-ph\]](#).
- [56] M. Ackermann et al. (Fermi-LAT), *Astrophys. J.* **857**, 49 (2018), [arXiv:1802.00100 \[astro-ph.HE\]](#).
- [57] S. W. Hawking, *Nature* **248**, 30 (1974).
- [58] D. N. Page, *Phys. Rev. D* **13**, 198 (1976).
- [59] J. H. MacGibbon and B. R. Webber, *Phys. Rev. D* **41**, 3052 (1990).
- [60] A. Arbey and J. Auffinger, *Eur. Phys. J. C* **79**, 693 (2019), [arXiv:1905.04268 \[gr-qc\]](#).
- [61] J. F. Navarro, C. S. Frenk, and S. D. M. White, *Astrophys. J.* **490**, 493 (1997), [arXiv:astro-ph/9611107](#).
- [62] P. F. de Salas, K. Malhan, K. Freese, K. Hattori, and M. Valluri, *JCAP* **10**, 037 (2019), [arXiv:1906.06133 \[astro-ph.GA\]](#).
- [63] M. M. Flores and A. Kusenko, *JCAP* **05**, 013 (2023), [arXiv:2108.08416 \[hep-ph\]](#).
- [64] T. H. Jung and T. Okui, *Phys. Rev. D* **110**, 115014 (2024), [arXiv:2110.04271 \[hep-ph\]](#).
- [65] R. Harnik, J. Kopp, and P. A. N. Machado, *JCAP* **07**, 026 (2012), [arXiv:1202.6073 \[hep-ph\]](#).
- [66] K. Agashe, J. H. Chang, S. J. Clark, B. Dutta, Y. Tsai, and T. Xu, *Phys. Rev. D* **108**, 023014 (2023), [arXiv:2212.11980 \[hep-ph\]](#).
- [67] G. Cowan, K. Cranmer, E. Gross, and O. Vitells, *Eur. Phys. J. C* **71**, 1554 (2011), [Erratum: *Eur.Phys.J.C* 73, 2501 (2013)], [arXiv:1007.1727 \[physics.data-an\]](#).
- [68] W. A. Rolke, A. M. Lopez, and J. Conrad, *Nucl. Instrum. Meth. A* **551**, 493 (2005), [arXiv:physics/0403059](#).
- [69] T. Bringmann, X. Huang, A. Ibarra, S. Vogl, and C. Weniger, *JCAP* **07**, 054 (2012), [arXiv:1203.1312 \[hep-ph\]](#).
- [70] M. Ackermann et al. (Fermi-LAT), *Phys. Rev. D* **91**, 122002 (2015), [arXiv:1506.00013 \[astro-ph.HE\]](#).

- [71] S. Clark, B. Dutta, Y. Gao, Y.-Z. Ma, and L. E. Strigari, [Phys. Rev. D **98**, 043006 \(2018\)](#), [arXiv:1803.09390 \[astro-ph.HE\]](#).